JOURNAL OF VIROLOGY, June 1996, p. 3449–3460 Vol. 70, No. 6
0022-538X/96/$04.00+0

Nucleoplasmic and Nucleolar Distribution of the Adenovirus IVa2 Gene Product

PIERRE LUTZ,[1] FRANCINE PUVION-DUTILLEUL,[2] YVES LUTZ,[1] AND CLAUDE KEDINGER[1]*

Institut de Génétique et de Biologie Moléculaire et Cellulaire (Centre National de la Recherche Scientifique/Institut National de la Santé et de la Recherche Médicale/ Université Louis Pasteur), F-67404 Illkirch Cedex C.U. de Strasbourg,[1] and UPR 9044 du CNRS (Institut Fédératif) Laboratoire de l'Organisation Fonctionnelle du Noyau, F-94801 Villejuif Cedex,[2] France

Received 27 December 1995/Accepted 6 March 1996

Sequence elements (DE) located downstream of the adenovirus major late promoter start site have previously been shown to be essential for the activation of this promoter after the onset of viral DNA replication. Two proteins (DEF-A and DEF-B) bind to these elements in a late-phase-dependent manner and contribute to this activation. DEF-B corresponds to a dimer of the adenovirus IVa2 gene product (pIVa2, 449 residues), while DEF-A is a heteromeric protein also comprising pIVa2. As revealed by specific immunofluorescence staining of infected cells, pIVa2 is targeted to the nucleus, where it distributes to both nucleoplasmic and nucleolar structures. We have identified the pIVa2 nuclear localization signal (NLS) as a basic peptide element at the C terminus of the protein (residues 432 to 449). An element essential for nucleolar localization (NuLS) has been mapped in the N-terminal part of pIVa2 (between residues 50 and 136). While NuLS activity is dependent upon an intact NLS, we show that both NLS and NuLS functions are independent of specific DNA-binding activity. As visualized by immunoelectron microscopy, pIVa2 is detected in the nucleoplasm at the level of the fibrillogranular network which is active in viral transcription. More surprisingly, pIVa2 accumulates within electron-dense amorphous inclusions found both in the nucleoplasm and in the nucleolus. Altogether, these results suggest that, besides controlling major late promoter transcription, pIVa2 serves additional, as yet unknown functions.

Adenoviruses (Ads) are icosahedral particles (about 80 nm in diameter) comprising 11 to 15 structural proteins and a double-stranded linear DNA molecule (19). The most commonly studied serotypes, Ad types 2 and 5 (Ad2 and Ad5), cause lytic infections in permissive cells, through infectious cycles of 36 to 40 h. Infection starts by receptor-mediated endocytosis (36) and subsequent viral DNA delivery to the cell nucleus (16). Immediate expression of the viral pre-early sequences (E1a) allows activation of the viral early genes which encode proteins involved in viral DNA replication (7, 19), proteins which counteract the immune system (55, 56), and proteins which interfere with cell growth control (35). Following the onset of viral DNA synthesis, the expression of genes (IVa2 and IX) belonging to the intermediate class of viral genes is turned on (4, 11, 25). Finally, activation of the major late promoter (MLP) leads to the production of the structural proteins that, together with the accumulated viral DNA, assemble into new virus particles.

Sequence elements (DE) located downstream of the MLP start site have been found to be essential for promoter activation (1, 20, 21, 24, 31–34). One of the proteins (DEF-B) which bind to these elements (between positions +85 and +120) and contribute to MLP activation has been identified as the product of the IVa2 gene (27, 53). This 449-residue protein (pIVa2), which is expressed after the onset of viral DNA replication and binds to its recognition site as a dimer, is the first adenoviral protein so far characterized that exhibits specific DNA-binding activity. Site-directed mutagenesis of pIVa2 has delineated two distinct domains (residues 50 to 100 and residues 357 to 449), each bearing sequence elements potentially capable of amphipathic helix formation, that are essential for specific sequence recognition (27). Immunofluorescence experiments have shown that pIVa2 is restricted to the nucleus and that it distributes both to the nucleoplasm and to the nucleolus (27).

Here we examine the nature of the sequence elements which are responsible for the efficient nuclear targeting and nucleolar retention of pIVa2. The subnuclear distribution of pIVa2 was also investigated at the ultrastructural level.

MATERIALS AND METHODS

Cells. HeLa cells were grown in suspension at a density of 10^6 cells per ml in Eagle medium supplemented with 5% calf serum or as monolayers in the presence of Dulbecco medium supplemented with 2.5% fetal calf serum and 2.5% newborn calf serum. Whole-cell extracts were prepared from uninfected cells or 20 h postinfection (hpi) with 10 PFU of Ad5 per cell as previously described (33). Monolayer COS-7 cells were grown in 5% newborn calf serum-supplemented Dulbecco medium.

Recombinant vectors. The IVa2 coding sequence and deleted versions lacking N-terminal (Δ1-50 and Δ1-136) or C-terminal (Δ441-449 and Δ357-449) amino acid residues were inserted into the p513 vector, a derivative of the pSG5 expression vector (17). The Δ441-449 mutation was obtained by creating a frameshift at residue 441 (insertion of 4 nucleotides at the corresponding position of the cDNA), resulting in the replacement of the natural residues 441 to 449 (AYRARKTPK) by the sequence PGLPRAQNP. The other deletions were constructed by oligonucleotide-directed mutagenesis (23). All constructs were verified by DNA sequencing.

A vector (pCHK-NLS.IVa2) expressing the putative nuclear localization signal (NLS) of pIVa2 in frame with the bacterial β-galactosidase coding sequence was

* Corresponding author. Mailing address: IGBMC, B.P. 163, 67404 Illkirch, France. Phone: (33) 88-65-34-46. Fax: (33) 88-65-32-01. Electronic mail address: kedinger@igbmc.u-strasbg.fr.

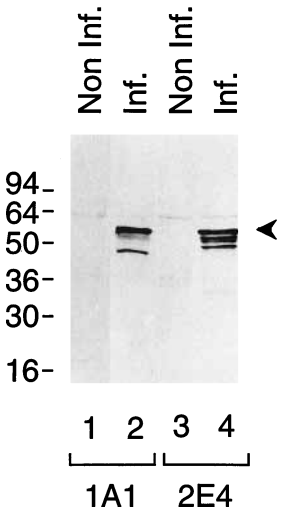

FIG. 1. Protein recognition pattern of pIVa2-specific MAbs. Uninfected HeLa cell extracts (Non Inf.) or Ad5-infected HeLa whole-cell extracts prepared 20 hpi (Inf.) were separated by SDS–10% PAGE and analyzed by immunoblotting with MAb1A1 or MAb2E4 as indicated. Prestained See Blue size markers (Novel Experimental Technology) are positioned on the left (kilodaltons). The arrowhead points to the expected location of pIVa2 (55 kDa).

constructed by inserting a synthetic oligonucleotide corresponding to residues 432 to 447 of pIVa2 into pCHK (50), a derivative of pCH110 (Pharmacia).

The pCHK-NLS.SV40 vector (gift of V. Schreiber and J. Menissier de Murcia) directs the expression of the simian virus 40 T-antigen NLS fused to the β-galactosidase protein (50).

Transfection. COS-7 cells were transfected by calcium phosphate coprecipitation (9) with recombinant DNA adjusted to 14 μg/9-cm-diameter petri dish with double-stranded pBluescript as the carrier DNA. After 36 h, the cells were harvested in ice-cold phosphate-buffered saline (PBS), pelleted, washed twice in the same buffer, and resuspended in extraction buffer (0.4 M KCl, 20 mM Tris-HCl [pH 7.9], 20% glycerol, 5 mM dithiothreitol, 0.4 mM phenylmethylsulfonyl fluoride). After two freeze-thaw cycles in liquid nitrogen, the resulting cell lysate was cleared by centrifugation for 15 min (4°C) at 10,000 × *g* and used for electrophoretic mobility shift assay (EMSA) analysis.

EMSA. Gel retardation assays were performed as previously described (33). Approximately 0.25 ng (15,000 cpm) of a ^{32}P-5′-end-labelled, synthetic double-stranded oligonucleotide, corresponding to the DE binding sites, was incubated with cell extracts in the presence of appropriate amounts of poly(dI-dC) as a nonspecific competitor. After 15 min at room temperature, the complexes were separated by nondenaturing 4.5% polyacrylamide gel electrophoresis (PAGE) (acrylamide-bisacrylamide, 80:1) at 4°C. Retardation competition experiments were carried out by preincubating the extracts with poly(dI-dC) and unlabelled competitor oligonucleotides for 15 min at room temperature before addition of the probe and further incubation (see above).

Antibodies and immunoblots. Hybridoma cell lines were obtained as previously described (27). Briefly, BALB/c mice were injected with bacterially synthesized recombinant pIVa2 or with a synthetic peptide (Pc) corresponding to residues 428 to 443 of pIVa2, coupled to ovalbumin. After immunization, mice were sacrificed and spleen cells were fused with Sp2/O-Ag14 myeloma cells. Hybridomas which secreted antibodies specifically recognizing pIVa2 were cloned twice on soft agar, resulting in the isolation of monoclonal antibody 1A1 (MAb1A1) (directed against an N-terminal domain of pIVa2 located roughly between residues 50 and 100, as revealed by gross epitope mapping) and MAb2E4 (directed against Pc). Immunoblot analysis of sodium dodecyl sulfate (SDS)-PAGE-separated proteins was performed as previously described (5).

Immunofluorescence. Monolayer HeLa cells, grown in Leighton tubes, were infected with Ad5 at 50 PFU per cell in serum-free medium. After 1 h of adsorption, this medium was changed with serum-supplemented medium. At various times after infection, cells were washed in PBS and treated for 4 min at room temperature with 2% formaldehyde in PBS. After fixation, the cells were permeabilized by two treatments with PT (PBS, 0.1% Triton X-100) of 10 min each. After a 30-min treatment with blocking solution (PBS, 2% nonfat dry milk), the cells were incubated for 1 h at room temperature with primary antibodies diluted in PT, washed thrice in PT, incubated with secondary antibodies for 1 h (at room temperature), and washed in PT. DNA was counterstained with Hoechst 33258 dye, and the preparations were mounted in glycerol-PBS (4:1) containing 5% propylgallate.

COS-7 cells, grown on glass coverslips, were transfected by calcium phosphate coprecipitation (9) with 1 μg of p513-IVa2 recombinant vectors or pCHK,

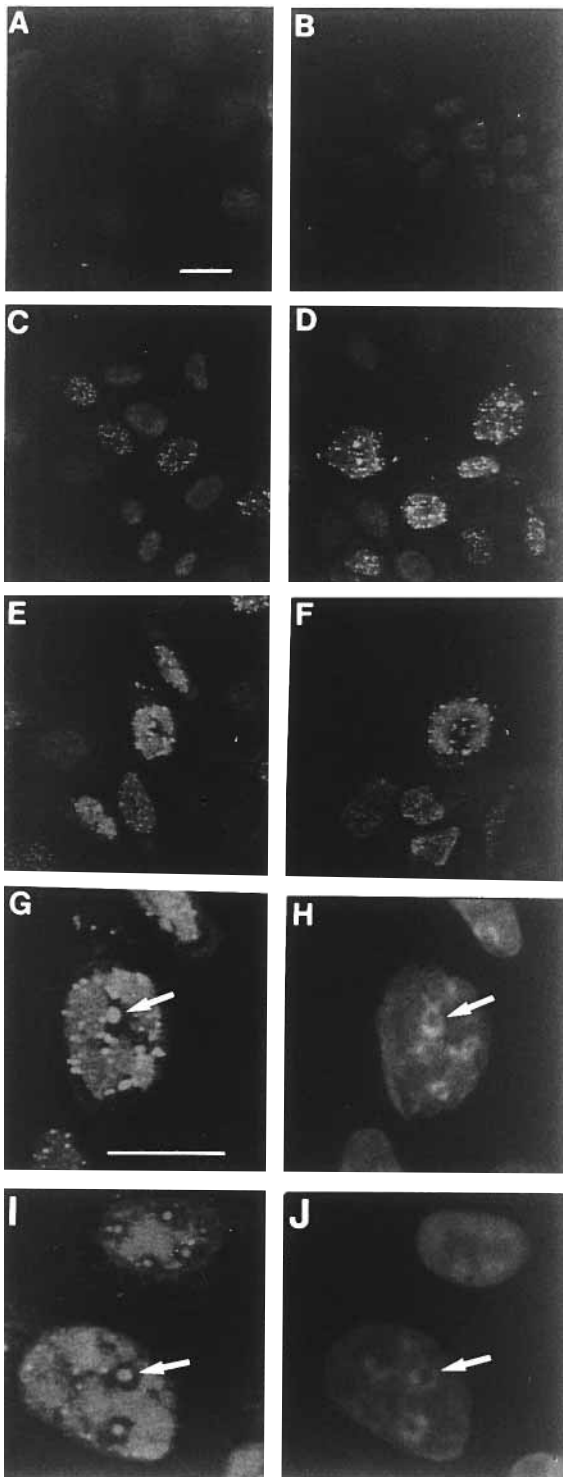

FIG. 2. Subcellular localization of pIVa2 during Ad5 infection. HeLa cells were mock infected (A) or infected with Ad5 at a multiplicity of 50 PFU per cell (B to J) and fixed at 8 (B), 12 (C), 16 (D), 20 (E and G to J), and 24 (F) hpi. After permeabilization, the cells were treated with MAb2E4 (A to G) or MAb1A1 (I) (undiluted hybridoma culture supernatant) and stained with Cy3-conjugated goat anti-mouse immunoglobulin G (Fcγ) (diluted 1:500). In panels H and J, the same cells as in panels G and I, respectively, were counterstained with Hoechst 33258 reagent. Enlargement (bars, 10 μm) was the same for panels A to F and 2.4-fold higher for panels G to J. Arrows indicate nucleoli.

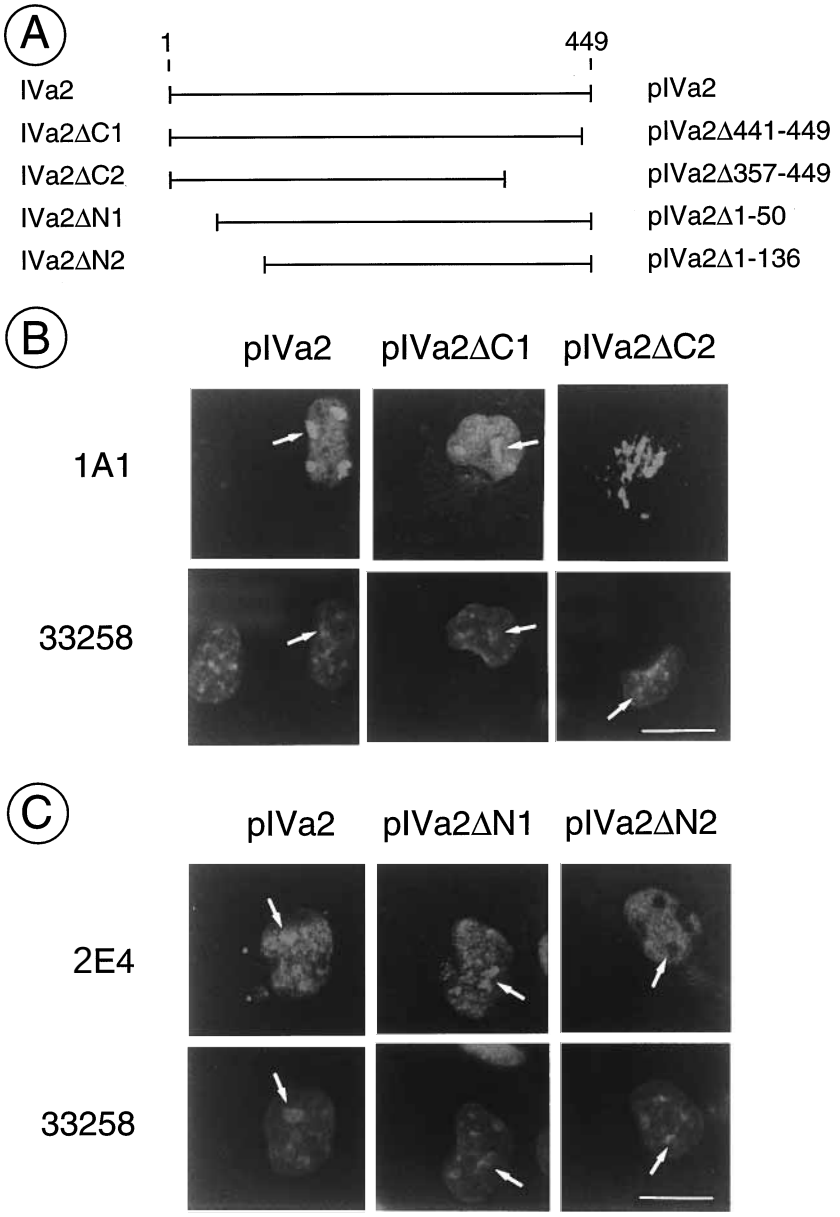

FIG. 3. Sequence elements involved in nuclear and nucleolar addressing of pIVa2. (A) Schematic representation of the IVa2 sequences encoded by the p513-based expression vectors used, with the wild-type pIVa2 on the top and C-terminally deleted (Δ441-449 [ΔC1] or Δ357-449 [ΔC2]) and N-terminally deleted (Δ1-50 [ΔN1] or Δ1-136 [ΔN2]) versions of the protein below. (B) Sequences involved in nuclear targeting: COS-7 cells were transfected with the indicated series of C-terminally truncated IVa2 constructs, permeabilized and treated with MAb1A1 (1A1), and stained with Cy3-conjugated goat anti-mouse immunoglobulins (Fcγ; diluted 1:1,000); the same cells were counterstained with Hoechst 33258 reagent (33258). (C) Sequences involved in nucleolar targeting: COS-7 cells were transfected with N-terminally deleted IVa2 recombinants as indicated, treated with MAb2E4 (2E4), and further processed as in panel B. Bars, 10 μm. Arrows indicate nucleoli.

together with 3.5 μg of double-stranded pBluescript carrier DNA per tube. The medium was changed after 20 h, and the next day, the cells were washed and treated for immunofluorescence, as described above.

Observations were made with a confocal microscope (Leica TCS4D) equipped with an argon-krypton laser and suitable barrier filters. A high-resolution film recorder was used to obtain photomicrographs.

Electron microscopy. HeLa cells grown in Eagle minimum essential medium supplemented with 5% newborn calf serum were seeded at a density of 5×10^5 cells per 5-cm-diameter petri dish. The next day, the cells (which were near confluency) were infected with Ad5 at 10 PFU per cell. Infected cultures were incubated for 12 and 17 h before fixation. Noninfected cells were used as controls.

Both noninfected and Ad5-infected cells were fixed for 1 h at 4°C with either 4% formaldehyde (Merck) or 1.6% glutaraldehyde (Taab Laboratory Equipment) in 0.1 M Sörensen phosphate buffer, pH 7.3. In some experiments, PBS was used instead of Sörensen phosphate buffer to maintain conditions similar to those used for photonic microscopy. After fixation, cells were scraped from the plates and centrifuged. Pellets were dehydrated in increasing concentrations of methanol and embedded in Lowicryl K4M (Chemische Werke Lowi) at a low temperature, according to the method of Roth (48). Polymerization was carried out at −30°C under long-wavelength UV light (Philips TL 6W fluorescent tubes) for 5 days. Ultrathin sections were collected on Formvar-carbon-coated gold grids (200 mesh) and stored until use.

For immunogold detection of pIVa2, grids bearing Lowicryl sections of noninfected and Ad5-infected HeLa cells were first placed on a 10-μl drop of a 5% bovine serum albumin solution in PBS for 30 min in order to minimize subsequent nonspecific binding of antibodies to the specimen. Grids were then floated for 1 h at room temperature on 10-μl drops of primary antibodies, either undiluted or diluted (1:10, 1:50, or 1:100 in PBS). After washing in PBS (15 min), the grids were floated on a 10-μl drop of goat anti-mouse immunoglobulin G (1:25 in PBS) conjugated to 10-nm gold particles (Biocell Research Laboratories). After a final PBS wash, the grids were rapidly rinsed in a stream of distilled

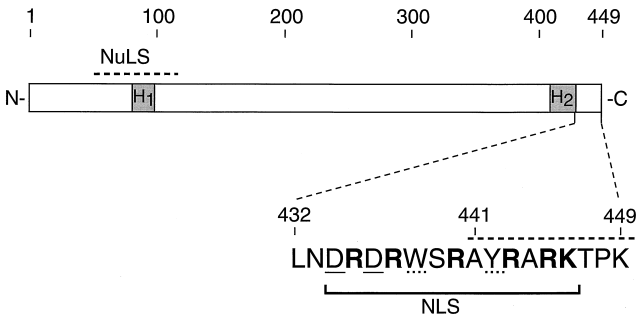

FIG. 4. Structural features of pIVa2. The sequence element exhibiting nuclear localization (NLS) properties is shown, positioned relative to the amino (N) and carboxy (C) termini of pIVa2 (449 residues). Basic residues are represented in boldface letters, acidic residues have solid underlines, and bulky residues have dotted underlines. Sequences predicted to form amphipathic helices and possibly involved in pIVa2 dimerization and DNA binding (27) are shown: H1 spanning residues 79 to 98 and H2 spanning residues 413 to 432. The residues that are essential for specific DNA binding are overlined (dashed line spanning residues 441 to 449) within the NLS. The domain encompassing the NuLS is delineated.

water, air dried, and stained for 10 min with 5% aqueous uranyl acetate. The specificity of the immunogold labelling was controlled by using normal mouse serum (1:10 in PBS) instead of the primary antibody.

RESULTS

Nucleoplasmic and nucleolar distribution of pIVa2, as revealed by immunofluorescence. Immunofluorescent staining experiments with pIVa2-specific antibodies had previously shown that the IVa2 gene product could be detected in infected cell nuclei from 12 hpi onwards, both in the nucleoplasm and within the nucleoli (27). While this initial study was carried out with an antibody (MAb1A1) directed against an N-terminal epitope of pIVa2, a similar analysis has been repeated with a distinct MAb (MAb2E4) directed against a C-terminal peptide of pIVa2. As a preliminary control, we verified that the two antibodies were specific and did not recognize any host cell protein. To this end, equal amounts of extracts prepared from uninfected and Ad5-infected cells were subjected to SDS-PAGE, transferred to nitrocellulose, and probed with each antibody. As shown in Fig. 1, both antibodies generated signals of similar intensities at the level of the full-length pIVa2 polypeptide (55 kDa) with infected-cell extracts. Additional bands corresponding to smaller polypeptides (most likely degradation products of pIVa2) were differentially detected with the two antibodies. By contrast, no band was detected with any antibody on mock-infected cell extracts, stressing the absence of any cross-reactivity of these antibodies with host cell polypeptides.

When applied to Ad5-infected cells that had been fixed and permeabilized at various times after infection, the two antibodies generated significantly different immunofluorescence patterns (Fig. 2). MAb1A1, in agreement with our earlier observation (27), brightly stained the nucleolus and produced a rather diffuse staining of the nucleoplasmic compartment (Fig. 2I). MAb2E4, on the other hand, revealed a speckled nuclear distribution detectable from 12 hpi (Fig. 2C), with a slightly delayed nucleolar staining that became clearly visible only after 16 hpi onward (Fig. 2D). At later times, a diffuse staining of the nucleoplasm superimposed on this dotted pattern also became apparent (Fig. 2E to G).

Since none of these antibodies exhibited background levels of nonspecific activity (Fig. 1), it is very unlikely that the differences in labelling patterns concerned proteins other than pIVa2. Rather, they probably reflected variations in epitope accessibility for the two antibodies. Thus, depending on its subnuclear localization, pIVa2 was probably differentially susceptible to antibody recognition: MAb1A1, although recognizing nucleoplasmic pIVa2, was more efficient in reaching pIVa2 in the nucleolus, whereas MAb2E4 preferentially targeted pIVa2 in nucleoplasmic bodies, revealed as speckles.

Identification of an NLS at the C terminus of pIVa2. In an attempt to map the signals which mediate pIVa2 nuclear localization, we constructed a set of pIVa2 cDNA deletion mutants, inserted in a eukaryotic cell expression vector (Fig. 3A). The recombinants were transfected into cultured cells, and the subcellular localizations of the corresponding overexpressed proteins were examined by indirect immunofluorescence (Fig. 3B). COS-7 cells were used in these experiments, because of the higher transfection efficiencies reached in these cells compared with that in HeLa cells. We previously verified that transfected pIVa2 was transcriptionally active in Ad-infected COS-7 cells (53) and that its subnuclear localization was the same in both cell lines (27). The largest C-terminal truncation (IVa2ΔC2), deleting sequences spanning residues 357 to 449, completely abolished nuclear accumulation of pIVa2, which was restricted to the cytoplasm. A comparison with reported NLS sequence compilations (6, 8, 12, 13) pointed to a basic sequence element (between residues 432 and 447 [Fig. 4]),

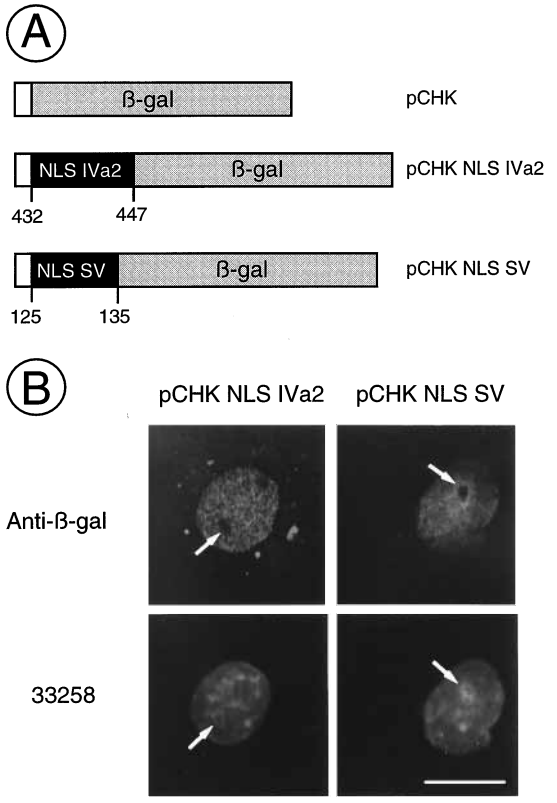

FIG. 5. Subcellular localization of a β-galactosidase fusion protein containing the putative NLS element of pIVa2. (A) The inserts of recombinant pCHK vectors encoding β-galactosidase, either alone or fused to the putative NLS of pIVa2 or to the simian virus 40 T antigen, are schematically depicted. (B) About 36 h following transfection of these vectors into COS-7 cells, cellular localization of the chimeric proteins was assessed by immunofluorescence microscopy. After permeabilization, the cells were treated with a MAb (Anti-β-gal) directed against β-galactosidase (diluted 1:2,000; Promega) and stained with Cy3-conjugated goat anti-mouse immunoglobulin G (Fcγ). The same cells were counterstained with Hoechst 33258 reagent (33258). Arrows indicate nucleoli. Bar, 10 μm.

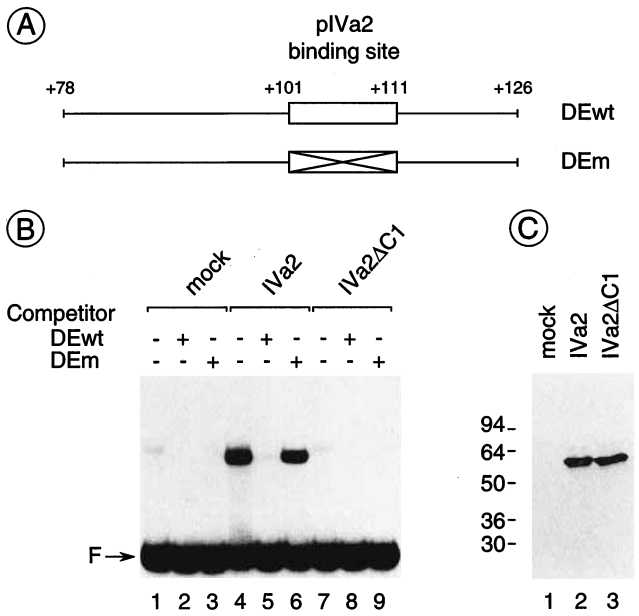

FIG. 6. Specific DNA binding of pIVa2 critically depends on the integrity of the C terminus of the protein. (A) Schematic representation of the oligonucleotides (coordinates with respect to the MLP start site at +1) used as the probe or competitor in EMSA reactions: the open box represents the pIVa2 binding site (DE2b; see reference 34 for details); DEwt corresponds to a double-stranded oligonucleotide with the wild-type DNA sequence; DEm differs from DEwt by alterations (crossed box) impairing specific complex formation, as previously described (34). (B) Recombinant expression vectors encoding the wild-type pIVa2 or the C-terminally deleted (Δ441-449 [ΔC1]) protein (Fig. 3 and 4) were transfected into COS-7 cells. "Mock" refers to cells that had been transfected with the unloaded p513 vector. Extracts prepared 36 h after transfection were analyzed by EMSA: 2-μl aliquots of extract were preincubated with 100 ng of poly(dI-dC) and 10 ng of DEm as nonspecific competitors and, where indicated, with a 20-fold molar excess of competitor oligonucleotide (DEwt or DEm) before addition of the DEwt probe. F points to the excess of free probe. (C) Aliquots corresponding to 10 μg of cell lysate were fractionated by SDS–10% PAGE, transferred to nitrocellulose, and probed with MAb1A1, which is directed against an epitope within the N-terminal portion of pIVa2.

unique within this C-terminal domain and conserved among a number of Ad serotypes (Swiss Prot accession numbers P03272, P03271, P03273, and P12539), with characteristics of a bona fide core NLS (6): (i) an NLS generally comprises at least six basic amino acid residues (boldfaced residues in Fig. 4), (ii) it usually contains residues with acidic or bulky side chains (underlined in Fig. 4), and (iii) it is often flanked by residues interrupting α-helices (helix H2, predicted by computer analysis on the N-terminal side of the presumptive NLS of pIVa2, is likely to be interrupted by the following D residue) (Fig. 4).

Consistent with a role of this element in nuclear localization, a deletion removing the C-terminal half of it (IVa2ΔC1) significantly reduced nuclear confinement of pIVa2, as revealed by increased cytoplasmic staining with specific antibodies (Fig. 3B). To further establish the central importance of the entire element in directing the nuclear accumulation of pIVa2, we generated a plasmid expressing residues 432 to 447 of pIVa2 in frame with the β-galactosidase coding sequence (pCHK-NLS.IVa2) (Fig. 5A). Expression of this construct after transfection into COS cells clearly resulted in nucleoplasmic accumulation of the hybrid protein (Fig. 5B), as revealed by the anti-β-galactosidase antibodies. Nonfused β-galactosidase was confined to the cytoplasm, whereas nontransfected cells were devoid of labelling (not shown).

Altogether, these results demonstrate conclusively that residues 432 to 447 of pIVa2 define a strong NLS, capable of mediating the nuclear localization of an unrelated protein. The efficiency of this element in targeting a protein to the nucleus was comparable to that of the NLS present in the simian virus 40 T antigen, as shown by the distribution pattern of the chimeric product of pCHK-NLS.SV (Fig. 5B).

The pIVa2 NLS overlaps with sequences essential for specific DNA-binding activity. Analysis of the pIVa2 sequence revealed that the NLS (comprising residues 432 to 447, as defined above) contains a high concentration of basic residues (38%) compared with the mean basic-residue content of the entire protein (12%). To examine the possibility that the basic residues clustered at the NLS position participate in the pIVa2 DNA-binding activity, we compared the ability of the IVa2 and IVa2ΔC1 proteins (Fig. 3A) to bind to the cognate DE element of the MLP (Fig. 6A). Cells were transfected with the corresponding recombinant vectors, and extracts were prepared and analyzed by EMSA (Fig. 6B). While equivalent amounts of each protein were recovered in the extracts (Fig. 6C), only the wild-type pIVa2 generated a specific retarded complex (Fig. 6B, lanes 4 to 6). Deletion of nine residues at the C terminus (residues 441 to 449) completely abolished specific DNA binding (lanes 7 to 9), indicating that these residues are critical components of the pIVa2 DNA-binding domain. That these essential residues are part of a larger element was initially suggested by deletion experiments showing that DNA-binding activity of pIVa2 was dependent not only on the C-terminal region of the protein but also on elements located between residues 50 and 100 (27). Whatever the precise nature of the pIVa2 DNA-binding domain is, it appears that the NLS activity is essentially independent from the DNA-binding activity, since a deletion which totally impaired specific DNA sequence recognition (ΔC1) did only slightly affect nuclear targeting (Fig. 3B).

Sequence elements spanning residues 50 to 136 are essential for nucleolar targeting of pIVa2. As illustrated by the specific labelling of subnuclear compartments with anti-pIVa2 antibodies (arrows in Fig. 2G and I and in top panels of Fig. 3B), substantial amounts of pIVa2 accumulate in the nucleoli. Towards the identification of the peptidic sequence element mediating its nucleolar localization, we investigated the subcellular distribution of a limited set of deletion variants of pIVa2. While a truncation removing the 50 N-terminal residues of pIVa2 (ΔN1) had no effect on pIVa2 localization, deletion of an additional 86 residues (ΔN2) completely abolished nucleolar localization of the corresponding IVa2 derivative (Fig. 3C). This observation indicates that an element essential for nucleolar targeting is present between amino acids 50 and 136. We have not further refined the mapping of this nucleolar localization signal (NuLS). However, in agreement with the current view of NuLS function, our results confirmed that nucleolar localization is dependent on an NLS, as an IVa2 mutant protein lacking NLS activity (ΔC2) was restricted to the cytoplasm and showed no detectable nucleolar targeting (Fig. 3B). On the other hand, we show that elements with NLS activity are unable by themselves to direct proteins to the nucleolus, as demonstrated by the lack of nucleolar staining in cells transfected with the pCHK-NLS.IVa2 and SV recombinants (Fig. 5B). Finally, it is noteworthy that a deletion (ΔC1) impairing DE2b complex formation had no marked effect on nucleolar accumulation (Fig. 3B), indicating that specific DNA binding of pIVa2 is not essential for NuLS function.

Localization of pIVa2 at the ultrastructural level. Ads induce dramatic changes in nuclear organization during the course of infection (summarized in Fig. 7). As revealed by electron microscopy, the earliest visible manifestation (at about 14 hpi) is the occurrence in the nucleoplasm of small

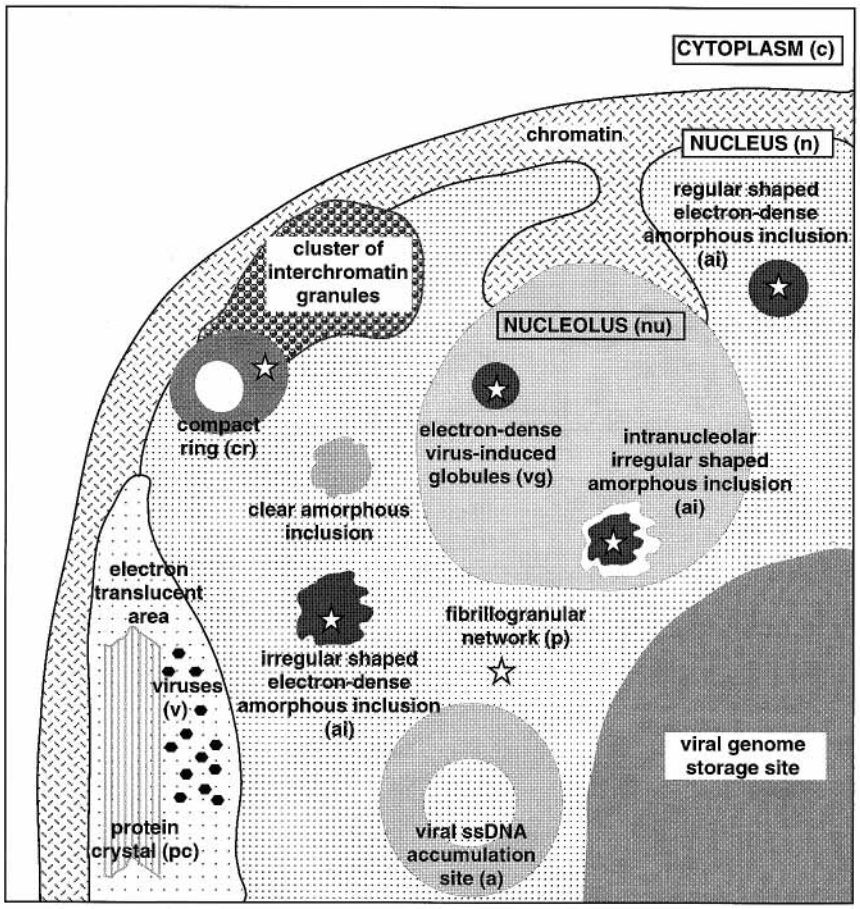

FIG. 7. Ad-induced alterations of the host cell nucleus during infection. The main structural alterations appearing during infection are schematically represented and named, with current abbreviations. Electron-dense amorphous inclusions, either round or less regular, were found both in the nucleoplasm or in the nucleolus: they have tentatively been given a single name (ai), their origin being presently unclear. Structures that were labelled after treatment with antibodies against pIVa2 are indicated with stars.

fibrillar masses that increase in size with time postinfection (43). These structures correspond to accumulation sites of single-stranded (ss) viral DNA and its associated 72-kDa ssDNA-binding protein (42). They are surrounded by the fibrillogranular network (also called the peripheral replicative zone), which fills the nucleus and pushes the host chromatin towards the nuclear border (2). This network is active in both viral DNA replication and transcription (43, 44, 46). The nonreplicating and nontranscribing viral genomes are stored in the central part of the nucleus, during late-phase progression. Nucleolar compaction arises at about 17 hpi, although a few nucleoli remained seemingly unchanged, even at 24 hpi. Late viral RNA accumulates in three types of nuclear structures: the fibrillogranular network, in which viral genomes are transcribed; clusters of interchromatin granules, which most likely participate in postsplicing events; and virus-induced compact rings, which essentially contain nonused portions of the primary transcripts resulting from differential polyadenylation site selection (39, 45, 46). Two additional types of inclusions (the electron-dense and clear amorphous inclusions), of yet unknown function, are found at late times within the fibrillogranular network. From 24 hpi onwards, the clear amorphous inclusions are found associated with an electron-translucent area containing protein crystals and virus particles (30, 40).

To identify the distinct structures targeted by pIVa2 during infection, we undertook a high-resolution immunocytochemistry study. Ultrathin sections of fixed Ad5-infected cells were probed with MAb1A1 or MAb2E4 and subsequently reacted with gold-conjugated anti-mouse antibodies. Identical results were obtained whether the cells had been fixed with glutaraldehyde or formaldehyde. However, the use of PBS instead of Sörensen buffer during fixation slightly enhanced the overall labelling, especially with MAb1A1. Irrespective of the fixation conditions, none of the MAbs used produced any detectable labelling of uninfected cells (not shown).

At 12 hpi, nuclei of infected cells looked apparently unchanged compared with those of uninfected cells (Fig. 8). A weak labelling was observed with MAb1A1 all over the nucleus (Fig. 8A), including the nucleolus and the virus-induced compact rings (0.5 μm in diameter) (Fig. 8B). A few gold particles were also visible in the cytoplasm (Fig. 8A). No significant labelling was obtained following treatment with MAb2E4 (not shown).

At 17 hpi, most nuclei were extensively modified (Fig. 9). Electron-dense virus-induced globules, rather spherical, were occasionally observed in nucleoli (Fig. 9A, C, and D). In some nuclear sections, more or less regularly shaped electron-dense amorphous inclusions were observed in the nucleoplasm (Fig. 9C and F and Fig. 10), close to (Fig. 9B, C, and E) or inside (Fig. 9E) the nucleolus. All virus-induced globule and

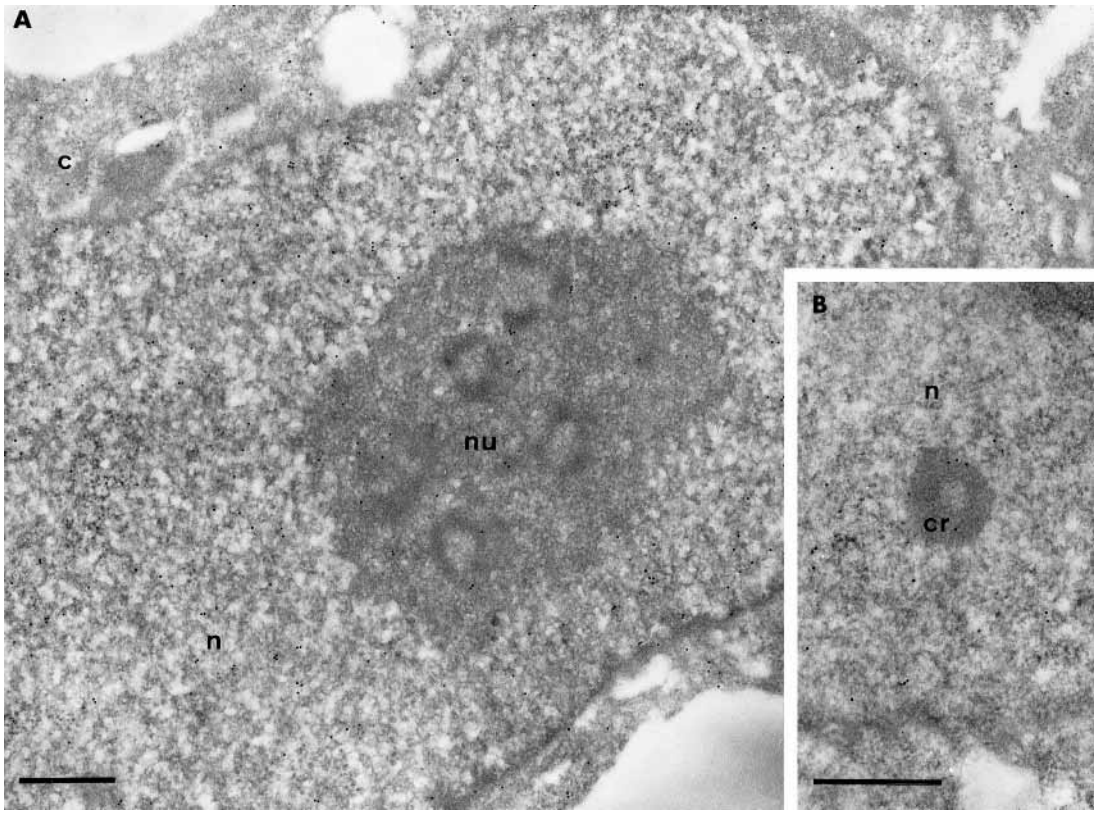

FIG. 8. Immunogold detection of pIVa2 at 12 hpi, using MAb1A1. Ad5-infected HeLa cells were fixed at 12 hpi with glutaraldehyde (A) or formaldehyde (B) in PBS buffer prior to Lowicryl embedding, slicing, immunoreaction (MAb1A1), and uranyl acetate staining of sections. (A) Gold particles are scattered through the cell but are significantly more abundant over the nucleus (c, cytoplasm; n, nucleoplasm; nu, nucleolus). (B) Gold particles are present over the intranuclear virus-induced compact ring (cr) and over the surrounding components of the nucleoplasm. Bars: 0.5 μm.

amorphous inclusion structures were intensely labelled following treatment with MAb2E4 (Fig. 9) and MAb1A1 (Fig. 10). By contrast, only MAb1A1 clearly labelled, though less intensely, the virus-induced compact rings, which were more frequent at 17 hpi (Fig. 10) than at 12 hpi (Fig. 8B), and the nuclear fibrillogranular network (Fig. 10). The viral ssDNA accumulation sites, protein crystals, and virus particles occasionally visible at this time postinfection were not labelled (Fig. 9F and 10).

DISCUSSION

The Ad IVa2 gene product (pIVa2) has previously been shown to interact with the downstream regulatory element (DE) of the MLP: pIVa2 binds as a homodimer (DEF-B) to the central part of this element and as a complex (DEF-A) with a distinct, yet unidentified protein(s) to either side of DEF-B (27, 53). Both complexes bind cooperatively to their target sequences and, together with upstream regulatory factors, contribute to the activation of the MLP (33). Since pIVa2 has no transcriptional activity on its own, it is assumed that it provides the promoter-binding activity, while its partner(s) supplies the activation function. Preliminary studies (27) had shown a clear nucleoplasmic distribution of pIVa2, in agreement with the functional properties of this protein and the nucleoplasmic location of transcribing viral DNA. Unexpectedly, these studies also revealed a significant level of targeting to the nucleolus, suggesting additional functions for pIVa2. To gain further insight into the mechanism of pIVa2 subnuclear localization, we have delineated the peptide sequence elements responsible for nuclear (NLS) and nucleolar (NuLS) targeting. In addition, we have examined, at the ultrastructural level, the fate of pIVa2 inside the nucleus during infection.

The pIVa2 NLS overlaps sequences that are essential for specific DNA binding. Deletion and fusion protein analyses allowed the identification of the NLS element involved in nuclear transportation of pIVa2. As already discussed, the structural characteristics of this element, which is located between residues 432 and 449, fit with those deduced from a compilation of a number of sequences with similar functions (6, 13). Interestingly, the pIVa2 NLS is part of a bipartite domain that spans residues 50 to 100 and residues 357 to 449 and that is responsible for specific DNA binding (27). Our present observations that nuclear localization of pIVa2 is completely independent from its binding to the DE sequence of the MLP clearly indicate, as previously suggested for other nuclear proteins (51), that an active transfer mechanism is involved. Furthermore, the fact that pIVa2 is directed to the nucleus when expressed from transfected vectors, in a noninfected-cell context, rules out any interaction of pIVa2 with a hypothetical viral karyophilic carrier protein.

In an earlier immunofluorescence study (54) Winter and D'Halluin reported that the distribution of pIVa2 was mainly cytoplasmic, although a slight shift towards the nucleus was observed only at later times. We do not know the reason for this discrepancy with our findings, but the identification of a strong NLS within pIVa2 tilts if anything, in favor of our conclusions.

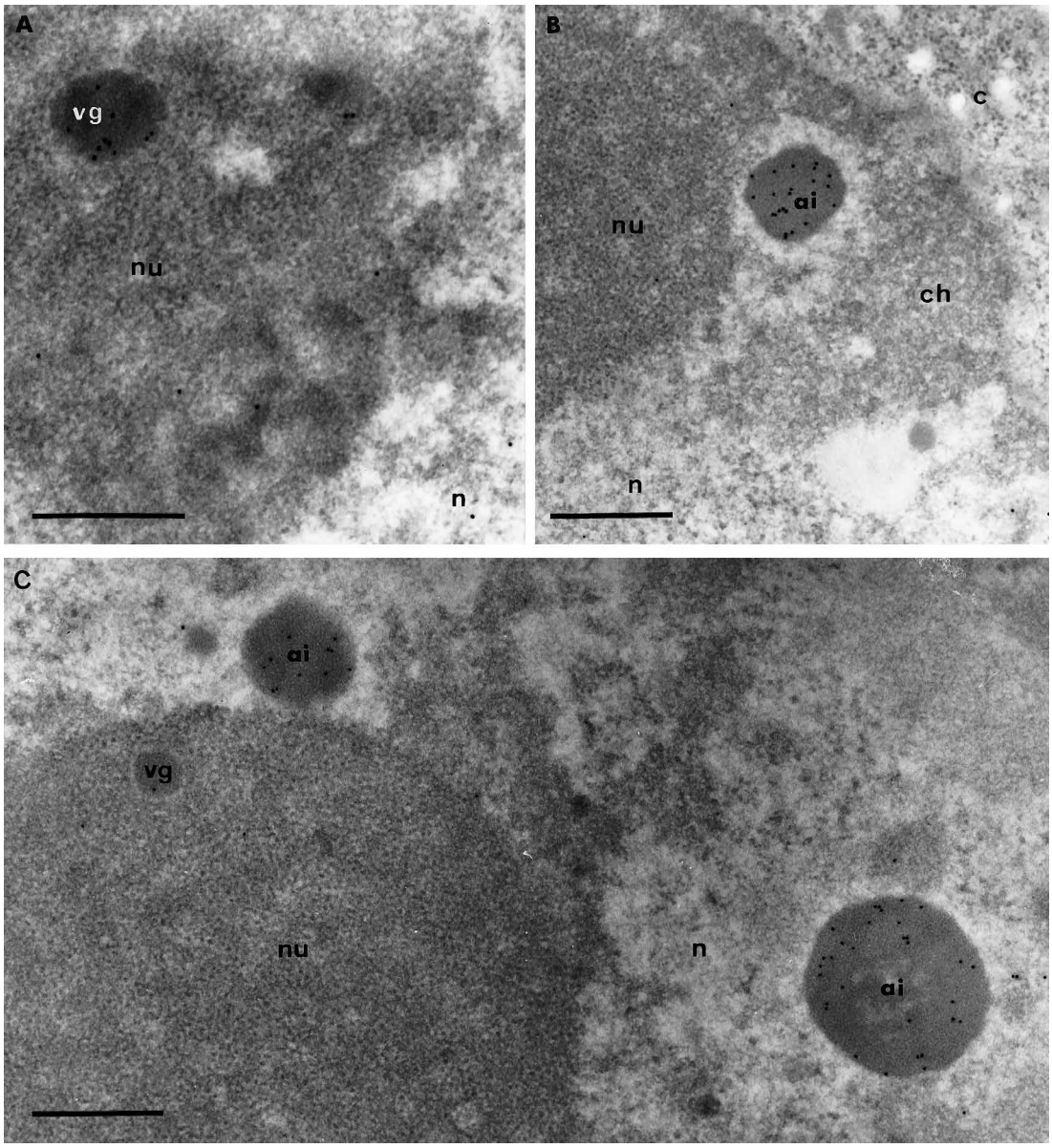

FIG. 9. Immunogold detection of pIVa2 at 17 hpi, using MAb2E4. Ad5-infected HeLa cells were fixed at 17 hpi with glutaraldehyde in Sörensen phosphate buffer, embedded, sliced, immunoreacted (MAb2E4), and uranyl acetate stained. (A to C) The intranucleolar virus-induced electron-dense globule (vg) in panel A is intensely labelled, whereas that in panel C, within a highly compacted nucleolus (nu), is smaller and only poorly labelled. The extranucleolar electron-dense amorphous inclusions (ai) in panels B and C are also intensely labelled, irrespective of their shape, irregular in panel B and spherical in panel C, and their location in the nucleoplasm (n). ch, condensed host chromatin. (D and E) Comparison at the same magnification of an intranucleolar virus-induced globule (vg) (D) and virus-induced electron-dense amorphous inclusions (ai) (E). (D) The intensely labelled vg element is closely surrounded by the nucleolar granules (g). (E) The three irregularly shaped ai elements are intensely labelled and surrounded by an unlabelled, electron-translucent halo. While ai1 and ai2 are near the nucleolus, ai3 is located within the nucleolus. (F) Part of a nucleus more advanced in infection, in which virus particles (v) and a protein crystal (pc) are present and entirely devoid of labelling. Gold particles are confined to the irregularly shaped ai structures. Bars: 0.5 μm.

The pIVa2 NuLS function does not depend on pIVa2 DNA-binding activity but requires NLS contribution. Rough mapping of the pIVa2 NuLS positions an element essential for this activity between residues 50 and 136, a region also known to comprise the N-terminal portion of the pIVa2 DNA-binding domain. Our results show (i) that nuclear entry occurs independently from nucleolar addressing, which can be impaired separately, and (ii) that impeding specific DNA binding of pIVa2 does not abolish nucleolar localization. The precise nature of the pIVa2 NuLS is presently unknown: the sequence encompassing the NuLS is not particularly rich in basic residues (about 1 arginine [R] or lysine [K] every 10 amino acids); no putative nucleolar RNA-binding motifs (glycine or arginine rich, acidic residue or serine rich, or containing HMG box repeats), previously described in a number of cellular proteins (10, 49, 57), could be identified within the entire pIVa2 sequence; and finally, preliminary transcription experiments, indicating that pIVa2 had no effect on ribosomal gene transcription (26), strongly suggested that pIVa2 does not bind to ribosomal promoter DNA.

Remarkably, a computer analysis (not shown) of the IVa2 peptide sequences from human (Ad2, Ad5, and Ad7; Swiss

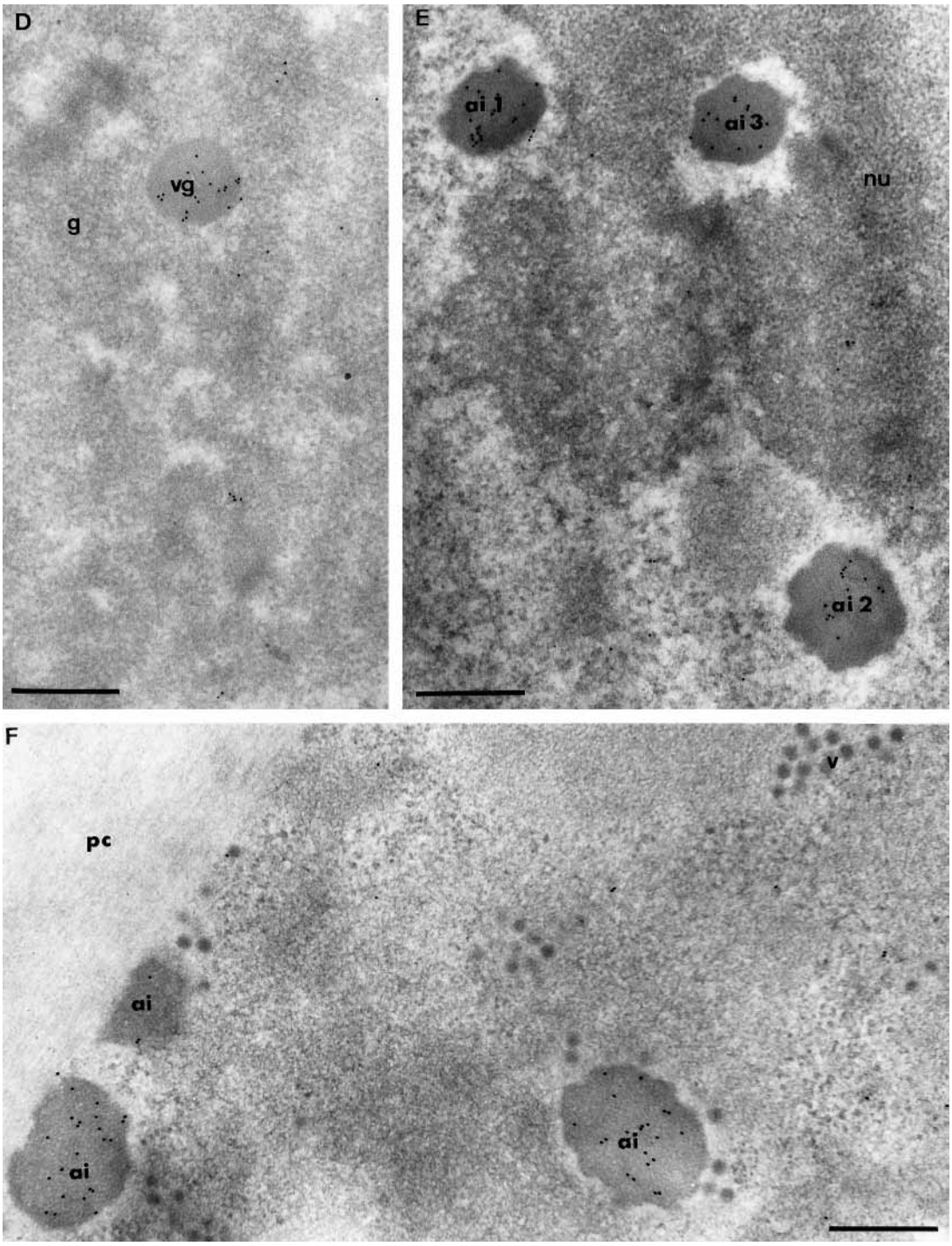

FIG. 9—*Continued.*

Prot accession numbers P03272, P03271, and P03273, respectively) and mouse (Ad1; Swiss Prot accession number P12539) serotypes revealed the conservation of two structural motifs (H1 and H2 in Fig. 4). While the sequence conservation of these elements (especially that of the most N-terminal one) is modest, both elements have the potential to fold into amphipathic α-helices. This observation further stresses the importance of the H1 and H2 structural elements. Although it is not known whether the mouse Ad IVa2 protein localizes to the nucleolus, this observation also suggests that the H1 motif, which lies within an otherwise poorly conserved region, is part of the pIVa2 NuLS.

There exists therefore the possibility that pIVa2 specifically interacts with a nucleolar protein harboring a retention signal and thus, once transported to the nucleus, will be sequestered in the nucleolar compartment. Such a model has initially been proposed for GAR1, a small nucleolar ribonucleoprotein-associated protein (15), although in this case NLS and NuLS

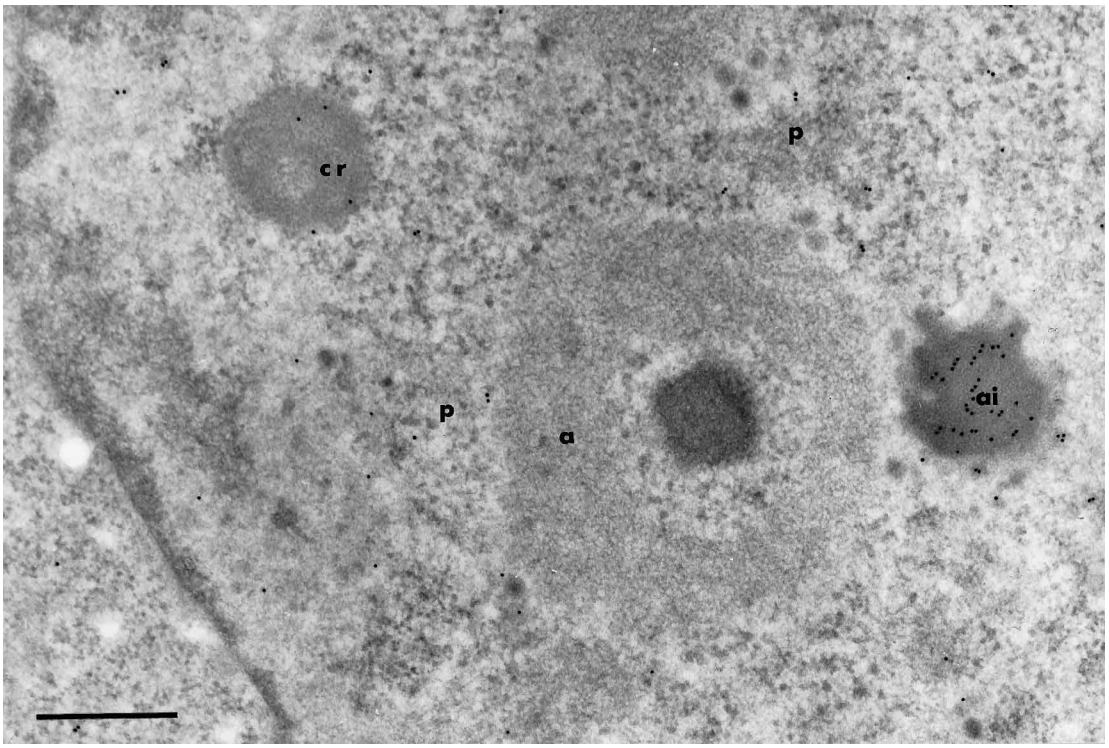

FIG. 10. Immunogold detection of pIVa2 at 17 hpi, using MAb1A1. Ad5-infected HeLa cells were treated as described in the legend to Fig. 8, but with MAb1A1. Gold particles are observed over the fibrillogranular network (p) and the compact ring (cr) but are most concentrated over the electron-dense amorphous inclusions (ai). The compact fibrillar mass, also designated the viral ssDNA accumulation site (a) and adopting here a ring-shaped structure, remains unlabelled. Bar: 0.5 μm.

could not be physically separated. It will be of interest to identify the nucleolar target(s) of pIVa2, if it exists.

Its nucleoplasmic and nucleolar distribution suggests that pIVa2 exerts multiple functions during infection. As visualized by electron microscopy of late Ad-infected cells, antibodies against pIVa2 most strongly labelled virus-induced electron-dense amorphous inclusions and globules located both in the nucleoplasm and in the nucleoli. A diffuse labelling is also observed, mainly over the nucleoplasmic fibrillogranular network. This pattern (schematized in Fig. 7) nicely correlates with the speckled distribution of pIVa2 revealed by specific immunofluorescence on top of a more uniform nucleoplasmic staining.

The localization of pIVa2 in the fibrillogranular area, initially identified as the site of viral DNA replication and transcription (43, 44, 46), is consistent with the contribution of this protein to MLP transcriptional activation. By contrast, the nature of the nucleoplasmic amorphous inclusion bodies is presently less clear: these structures have been reported to contain neither viral DNA nor RNA (52) but to react with antibodies against components of cellular heterogeneous nuclear ribonucleoprotein particles (30), suggesting a storage function for proteins participating in RNA maturation and/or transport. Thus, the elevated amounts of pIVa2 detected within these structures may just reflect the stockpiling of this protein. Alternatively, the presence of pIVa2 in distinct nuclear particles raises the interesting possibility that pIVa2 exerts additional functions besides controlling MLP activation.

This conclusion is in fact further supported by the finding of pIVa2 in similar electron-dense structures inside the nucleoli (amorphous inclusions and virus-induced globules), the role of which has not yet been established. Other viral regulatory proteins have been reported to localize to the nucleolus. Among these are the U_s11 gene products of herpes simplex virus type 1 (29, 38, 47), the Rex protein of human T-cell leukemia virus type 1 (22), and the Rev protein of human immunodeficiency virus type 1 (37). It will be important to determine whether pIVa2, like the above-mentioned proteins, can modulate the accumulation of viral or cellular transcripts by acting at some posttranscriptional level. It may be relevant in this respect that pIVa2 was reproducibly detected in association with the compact ring structures found in the nucleoplasm and which have been attributed to contain nonpolyadenylated RNA molecules (3, 39).

Finally, it is worth recalling that anti-pIVa2 antibodies did not significantly label the electron-translucent area containing protein crystals and virus particles, in contrast to antibodies directed against the product of the Ad IX gene (pIX) (28) or against the Ad L1 52- and 55-kDa proteins (18), which intensely labelled this region. The pIX protein, which is a shell component of the mature virus, has been proposed to play a connecting function between the hexons (14). The L1 52- and 52-kDa proteins seem to be absent from mature virions but are thought to play a transient role in assembly of the Ad particle (18). It is unlikely therefore that pIVa2 has any of these properties: it is not a virion component and probably does not participate in the maturation of the virus. The use of a virus deleted for the IVa2 coding region, together with the transfection of vectors expressing wild-type or truncated pIVa2, will be most helpful to clarify the putative multiple functions of this protein.

ACKNOWLEDGMENTS

We thank R. Gopalkrishnan for critical reading of the manuscript, C. Hauss and E. Pichard for expert technical assistance, the IGBMC

cell culture staff for providing cells, and the chemistry staff for preparing oligonucleotides and sequencing DNA. Many thanks go to V. Schreiber for the gift of plasmids, J. L. Vonesch for confocal microscopy, and B. Boulay and J.-M. Lafontaine for artwork. We also thank all the members of our team, especially J. Acker, H. Boeuf, B. Chatton, and M. Vigneron, for stimulating discussions.

This work was supported by funds from the Institut National de la Santé et de la Recherche Médicale, the Centre National de la Recherche Scientifique, the Centre Hospitalier Universitaire Régional, the Association pour la Recherche sur le Cancer, the Ligue Nationale contre le Cancer, and the Human Frontier Science Program (RG-496/93).

REFERENCES

1. **Alonso-Caplen, F. V., M. G. Katze, and R. M. Krug.** 1988. Efficient transcription, not translation, is dependent on adenovirus tripartite leader sequences at late times of infection. J. Virol. **62:**1606–1616.
2. **Besse, S., and F. Puvion-Dutilleul.** 1994. Compartmentalization of cellular and viral DNAs in adenovirus type 5 infection as revealed by ultrastructural in situ hybridization. Chromosome Res. **2:**123–135.
3. **Besse, S., and F. Puvion-Dutilleul.** 1995. Anchorage of adenoviral RNAs to clusters of interchromatin granules. Gene Expr. **5:**79–92.
4. **Binger, M. H., and S. J. Flint.** 1984. Accumulation of early and intermediate mRNA species during subgroup C adenovirus productive infections. Virology **136:**387–403.
5. **Bocco, J. L., B. Reimund, B. Chatton, and C. Kedinger.** 1993. Rb may act as a transcriptional co-activator in undifferentiated F9 cells. Oncogene **8:**2977–2986.
6. **Boulikas, T.** 1994. Putative nuclear localization signals (NLS) in protein transcription factors. J. Cell. Biochem. **55:**32–58.
7. **Challberg, M. D., and T. J. Kelly.** 1989. Animal virus DNA replication. Annu. Rev. Biochem. **58:**671–717.
8. **Chelsky, D., R. Ralph, and G. Jonak.** 1989. Sequence requirements for synthetic peptide-mediated translocation to the nucleus. Mol. Cell. Biol. **9:**2487–2492.
9. **Chen, C., and H. Okayama.** 1987. High-efficiency transformation of mammalian cells by plasmid DNA. Mol. Cell. Biol. **7:**2745–2752.
10. **Creancier, L., H. Prats, C. Zanibellato, F. Amalric, and B. Bugler.** 1993. Determination of the functional domains involved in nucleolar targeting of nucleolin. Mol. Biol. Cell **4:**1239–1250.
11. **Crossland, L. D., and H. J. Raskas.** 1983. Identification of adenovirus genes that require template replication for expression. J. Virol. **46:**737–748.
12. **Dingwall, C., and R. A. Laskey.** 1986. Protein import into the cell nucleus. Annu. Rev. Cell Biol. **2:**367–390.
13. **Dingwall, C., and R. A. Laskey.** 1991. Nuclear targeting sequences—a consensus? Trends Biochem. Sci. **16:**478–481.
14. **Furcinitti, P. S., J. van Oostrum, and R. M. Burnett.** 1989. Adenovirus polypeptide IX revealed as capsid cement by difference images from electron microscopy and crystallography. EMBO J. **8:**3563–3570.
15. **Girard, J. P., C. Bagni, M. Caizergues-Ferrer, F. Amalric, and B. Lapeyre.** 1994. Identification of a segment of the small nucleolar ribonucleoprotein-associated protein GAR1 that is sufficient for nucleolar accumulation. J. Biol. Chem. **269:**18499–18506.
16. **Greber, U. F., M. Willetts, P. Webster, and A. Helenius.** 1993. Stepwise dismantling of adenovirus 2 during entry into cells. Cell **75:**477–486.
17. **Green, S., I. Issemann, and E. Sheer.** 1988. A versatile in vivo and in vitro eukaryotic expression vector for protein engineering. Nucleic Acids Res. **16:**369.
18. **Hasson, T. B., D. A. Ornelles, and T. Shenk.** 1992. Adenovirus L1 52- and 55-kilodalton proteins are present within assembling virions and colocalize with nuclear structures distinct from replication centers. J. Virol. **66:**6133–6142.
19. **Horwitz, M. S.** 1990. Adenoviridae and their replication, p. 1679–1721. *In* B. N. Fields, D. M. Knipe, et al. (ed.), Virology, 2nd ed. Raven Press Ltd., New York.
20. **Jansen-Durr, P., H. Boeuf, and C. Kedinger.** 1988. Replication-induced stimulation of the major late promoter of adenovirus is correlated to the binding of a factor to sequences in the first intron. Nucleic Acids Res. **16:**3771–3786.
21. **Jansen-Durr, P., G. Mondesert, and C. Kedinger.** 1989. Replication-dependent activation of the adenovirus major late promoter is mediated by the increased binding of a transcription factor to sequences in the first intron. J. Virol. **63:**5124–5132.
22. **Kalland, K. H., E. Langhoff, H. J. Bos, H. Gottlinger, and W. A. Haseltine.** 1991. Rex-dependent nucleolar accumulation of HTLV-I mRNAs. New. Biol. **3:**389–397.
23. **Kunkel, T. A., J. D. Roberts, and R. A. Zakour.** 1987. Rapid and efficient site-specific mutagenesis without phenotypic selection. Methods Enzymol. **154:**367–382.
24. **Leong, K., W. Lee, and A. J. Berk.** 1990. High-level transcription from the adenovirus major late promoter requires downstream binding sites for late-phase-specific factors. J. Virol. **64:**51–60.
25. **Lewis, J. B., H. Esche, J. E. Smart, B. W. Stillman, M. L. Harter, and M. B. Mathews.** 1980. Organization and expression of the left third of the genome of adenovirus. Cold Spring Harbor Symp. Quant. Biol. **44:**493–508.
26. **Lutz, P.** Unpublished data.
27. **Lutz, P., and C. Kedinger.** 1996. Properties of the adenovirus IVa2 gene product, an effector of late-phase-dependent activation of the major late promoter. J. Virol. **70:**1396–1405.
28. **Lutz, P., and F. Puvion-Dutilleul.** Unpublished data.
29. **MacLean, C. A., F. J. Rixon, and H. S. Marsden.** 1987. The products of gene US11 of herpes simplex virus type 1 are DNA-binding and localize to the nucleoli of infected cells. J. Gen. Virol. **68:**1921–1937.
30. **Mahe, D., R. Roussev, Y. Lutz, F. Puvion-Dutilleul, and J. P. Fuchs.** 1995. Two hnRNP-associated proteins share common structural features with the adenoviral 72-kDa protein. Exp. Cell Res. **216:**1–12.
31. **Mansour, S. L., T. Grodzicker, and R. Tjian.** 1986. Downstream sequences affect transcription initiation from the adenovirus major late promoter. Mol. Cell. Biol. **6:**2684–2694.
32. **Mason, B. B., A. R. Davis, B. M. Bhat, M. Chengalvala, M. D. Lubeck, G. Zandle, B. Kostek, S. Cholodofsky, S. Dheer, and K. Molnar-Kimber.** 1990. Adenovirus vaccine vectors expressing hepatitis B surface antigen: importance of regulatory elements in the adenovirus major late intron. Virology **177:**452–461.
33. **Mondesert, G., and C. Kedinger.** 1991. Cooperation between upstream and downstream elements of the adenovirus major late promoter for maximal late phase-specific transcription. Nucleic Acids Res. **19:**3221–3228.
34. **Mondesert, G., C. Tribouley, and C. Kedinger.** 1992. Identification of a novel downstream binding protein implicated in late-phase-specific activation of the adenovirus major late promoter. Nucleic Acids Res. **20:**3881–3889.
35. **Moran, E.** 1993. Interaction of adenoviral proteins with pRB and p53. FASEB J. **7:**880–885.
36. **Nemerow, G. R., D. A. Cheresh, and T. J. Wickham.** 1994. Adenovirus entry into host cells: a role for α_v integrins. Trends Cell Biol. **4:**52–55.
37. **Nosaka, T., T. Takamatsu, Y. Miyazaki, K. Sano, A. Sato, S. Kubota, M. Sakurai, Y. Ariumi, M. Nakai, S. Fujita, and M. Hatanaka.** 1993. Cytotoxic activity of rev protein of human immunodeficiency virus type 1 by nucleolar dysfunction. Exp. Cell Res. **209:**89–102.
38. **Puvion-Dutilleul, F.** 1987. Localization of viral-specific 21 kDa protein in nucleoli of herpes simplex infected cells. Eur. J. Cell Biol. **43:**487–498.
39. **Puvion-Dutilleul, F., J. P. Bachellerie, N. Visa, and E. Puvion.** 1994. Rearrangements of intranuclear structures involved in RNA processing in response to adenovirus infection. J. Cell Sci. **107:**1457–1468.
40. **Puvion-Dutilleul, F., M. K. Chelbialix, M. Koken, F. Quignon, E. Puvion, and H. de Thé.** 1995. Adenovirus infection induces rearrangements in the intranuclear distribution of the nuclear body-associated PML protein. Exp. Cell Res. **218:**9–16.
41. **Puvion-Dutilleul, F., and M. E. Christensen.** 1993. Alterations of fibrillarin distribution and nucleolar ultrastructure induced by adenovirus infection. Eur. J. Cell Biol. **61:**168–176.
42. **Puvion-Dutilleul, F., J. Pedron, and C. Cajean-Feroldi.** 1984. Identification of intranuclear structures containing the 72K DNA-binding protein of human adenovirus type 5. Eur. J. Cell Biol. **34:**313–322.
43. **Puvion-Dutilleul, F., and E. Puvion.** 1990. Replicating single-stranded adenovirus type 5 DNA molecules accumulate within well-delimited intranuclear areas of lytically infected HeLa cells. Eur. J. Cell Biol. **52:**379–388.
44. **Puvion-Dutilleul, F., and E. Puvion.** 1990. Analysis by in situ hybridization and autoradiography of sites of replication and storage of single- and double-stranded adenovirus type 5 DNA in lytically infected HeLa cells. J. Struct. Biol. **103:**280–289.
45. **Puvion-Dutilleul, F., and E. Puvion.** 1991. Sites of transcription of adenovirus type 5 genomes in relation to early viral DNA replication in infected HeLa cells. A high resolution in situ hybridization and autoradiographical study. Biol. Cell **71:**135–147.
46. **Puvion-Dutilleul, F., R. Roussev, and E. Puvion.** 1992. Distribution of viral RNA molecules during the adenovirus type 5 infectious cycle in HeLa cells. J. Struct. Biol. **108:**209–220.
47. **Roller, R. J., and B. Roizman.** 1992. The herpes simplex virus 1 RNA binding protein US11 is a virion component and associates with ribosomal 60S subunits. J. Virol. **66:**3624–3632.
48. **Roth, J.** 1989. Postembedding labeling on Lowicryl K4M tissue sections: detection and modification of cellular components. Methods Cell Biol. **31:**513–551.
49. **Schmidt-Zachmann, M. S., and E. A. Nigg.** 1993. Protein localization to the nucleolus: a search for targeting domains in nucleolin. J. Cell Sci. **105:**799–806.
50. **Schreiber, V., G. de Murcia, and J. Ménissier-de Murcia.** 1994. A eukaryotic expression vector for the study of nuclear localization signals. Gene **150:**411–412.
51. **Silver, P. A.** 1991. How proteins enter the nucleus. Cell **64:**489–497.
52. **Thiry, M., and F. Puvion-Dutilleul.** 1995. Differential distribution of single-stranded DNA, double-stranded DNA and RNA in adenovirus-induced in-

tranuclear regions of HeLa cells. J. Histochem. Cytochem. **43:**749–759.
53. **Tribouley, C., P. Lutz, A. Staub, and C. Kedinger.** 1994. The product of the adenovirus intermediate gene IVa2 is a transcriptional activator of the major late promoter. J. Virol. **68:**4450–4457.
54. **Winter, N., and J. C. D'Halluin.** 1991. Regulation of the biosynthesis of subgroup C adenovirus protein IVa2. J. Virol. **65:**5250–5259.
55. **Wold, W. S., and L. R. Gooding.** 1991. Region E3 of adenovirus: a cassette of genes involved in host immunosurveillance and virus-cell interactions. Virology **184:**1–8.
56. **Wold, W. S., T. W. Hermiston, and A. E. Tollefson.** 1994. Adenovirus proteins that subvert host defenses. Trends Microbiol. **2:**437–443.
57. **Yan, C., and T. Melese.** 1993. Multiple regions of NSR1 are sufficient for accumulation of a fusion protein within the nucleolus. J. Cell Biol. **123:**1081–1091.